AD-A078 324 FLORIDA STATE UNIV TALLAHASSEE F/G 4/2
LABORATORY MODELLING OF OCEANIC RESPONSE TO MONSOONAL WINDS.(U)
DEC 77 R KRISHNAMURTI N00014-75-C-0877
UNCLASSIFIED TR-15 NL

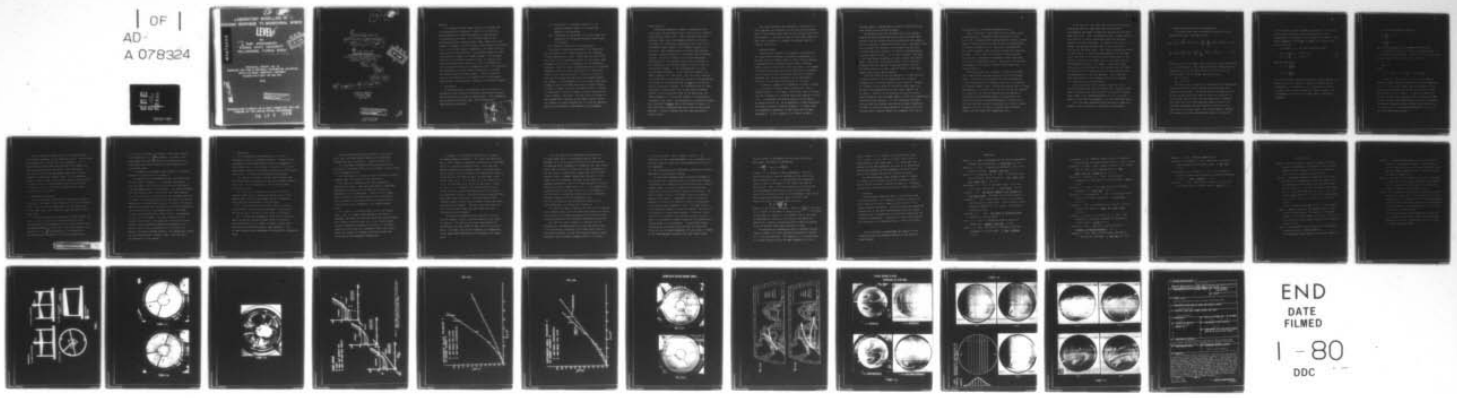

END
DATE FILMED
1-80
DDC

(12)

LABORATORY MODELLING OF OCEANIC RESPONSE TO MONSOONAL WINDS

LEVEL II

BY
RUBY KRISHNAMURTI
FLORIDA STATE UNIVERSITY
TALLAHASSEE, FLORIDA 32306

TECHNICAL REPORT NO. 15
APPROVED FOR PUBLIC RELEASE; DISTRIBUTION UNLIMITED
OFFICE OF NAVAL RESEARCH CONTRACT
N-00014-75-C-0877 NR 062-547

1978

79 12 3 039

(12)

(6) LABORATORY MODELLING OF OCEANIC RESPONSE TO MONSOONAL WINDS.

(9) Technical rept.,

by

(10) Ruby Krishnamurti
Department of Oceanography and
Geophysical Fluid Dynamics Institute
Florida State University
Tallahassee, Florida 32306

(11) Dec 77

(12) 38

(14) TR-15

(15) N0014-75-C-0877

IUTAM-IUGG SYMPOSIUM
on Monsoon Dynamics
IIT, Delhi, India
Dec. 1977

139850

Abstract

In a laboratory model ocean, fluid in a rotating tank of varying depth is subjected to various stress patterns which simulate both steady and seasonally varying winds, including monsoonal winds. For a certain range of the governing parameters (Rossby number, Ekman number and Froude number), a homogeneous fluid displays steady westward intensified flow. For the same range of parameters a two-layer fluid can have baroclinic instabilities. The parameter range for these instabilities is mapped in a regime diagram. The northward transport of the western boundary current is measured as it varies with imposed wind-stress curl, and is compared with the corresponding values in a homogeneous fluid. The conditions for surfacing of the lower layer is measured as it varies with Rossby number and Froude number. Finally a movie is shown of the response of a two layer fluid to periodically varying winds corresponding to southwest and northeast monsoons.

1. Introduction

A laboratory model of wind-driven ocean circulation is described in which various wind-stress patterns are simulated which drive fluid in a tank of varying depth. Both homogeneous and two-layer fluids were used. The following three experiments are described:

(i) measurement of northward transport in the western boundary current as it varies with magnitude of wind-stress.

(ii) conditions for surfacing of the lower layer and separation of the western boundary current from the boundary.

(iii) periodic forcing of a two-layer model.

The first of these was motivated by the observation that the oceans effect a major portion of the transport of heat from equator to pole. Vonder Haar and Oort (1973) have shown that the poleward transport by the oceans, when averaged over latitude, is comparable to the atmospheric transport. However, unlike the atmosphere which is primarily thermally driven, the upper oceans are to a large extent driven by the atmospheric winds. These winds change not only with the seasons but also with the changing climate. For example T. N. Krishnamurti, in this volume, shows major changes in air flow pattern from years of normal rainfall to years of drought over India and North Africa. It would be interesting to know the change in oceanic transport for a given change in the winds. Not only does this change in the poleward heat transport by the oceans directly affect the climate at a given latitude but it is also an important factor in the question of maintenance of the permanent

Arctic sea ice.

The second experiment, related to surfacing of the lower layer, was performed to test a theory due to Professor George Veronis (1973, 1977). For a two-layer model with quiescent lower layer, his argument proceeds as follows. In a region of anticyclonic wind-stress curl (such as the subtropical North Atlantic), the Sverdrup transport is to the south. Mass balance across a latitude line requires an equal northward transport in the region near the western boundary. This would require, for the geostrophically balanced part of the transport alone, that the height of the interface at the western boundary be equal to that at the eastern boundary. To this consideration, one must add the Ekman transport. In the Trade wind regions, the Ekman transport is to the north. Thus the return transport on the west must be less than that required by the geostrophic flow alone, so the interface must be lower at the western than at the eastern boundary. If surfacing occurs at these latitudes, it would occur first on the eastern boundary. However, in the anticyclonic part of the Westerlies, the Ekman transport is to the South, adding to the geostrophic transport to the south. The interface at the western boundary must therefore by higher than at the eastern boundary. At these latitudes, surfacing would occur first on the western boundary. A similar argument has also been presented by Parsons (1969).

The third experiment was performed to simulate, in a very rough way, the response of a sea (such as the Arabian Sea) to time varying winds (such as the south-west and north-east monsoons.) The spin-up time of a two-layer laboratory model can be adjusted to resemble the response time of a tropical ocean basin.

2. Laboratory model

Certain gross features of the general circulation of the oceans can be modelled in laboratory experiments, as has been shown by Stommel, Arons, & Faller (1958), Pedlosky & Greenspan (1967), Beardsley (1969), Baker & Robinson (1969), Veronis (1973), Hart (1975) and others. For example, a constant wind stress curl can be simulated by a rotating lid in contact with the fluid, and variation of Coriolis parameter with latitude (β-effect) can be simulated by variation of fluid depth with location in the tank.

A schematic diagram of the apparatus is shown in figure 1. A circular cylindrical tank is divided into three separate basins: a 180^0 basin, a 120^0 basin, and a 60^0 basin. The tank is placed on a rotating table whose angular velocity is Ω. A cone-shaped lid rotates relative to the tank at an angular velocity $\Delta\Omega$. As in Beardsley's (1969) experiments this model possesses a western boundary. It differs from his homogeneous experiments in that these are two-layer experiments. In this respect, it is similar to Hart's

two-layer models. However Hart's studies, directed to polar ocean basins, had no western boundary.

The physical basis for the model lies in the analogy between the vortex stretching by flow across constant depth contours, and the relative vorticity produced by the oceanic flow to latitudes of different Coriolis force. Greenspan (1968) has elucidated the difference in the flows that may arise in closed containers having or not having closed geostrophic (constant depth) contours. It is seen in figure 1 that each of the three basins possesses no closed contours of constant depth. The nature of the steady driven flow is completely different from the case with closed geostrophic contours. The interior flow is a slow, order $E^{\frac{1}{2}}$ (where E is the Ekman number) drift across depth contours.

Since the speed on the top boundary is a linear function of radial distance, the top Ekman layer has a constant divergence with a vertical velocity w_E of order $E^{\frac{1}{2}}$. Because the interior flow is order $E^{\frac{1}{2}}$, the bottom Ekman layer, for the case of a homogeneous fluid, has a much smaller flux of order E. However, if the interior flow would be across depth contours at just the right speed v so that the orographically induced vertical velocity $w = v \tan \alpha$ balances the Ekman flux w_E, then the interior velocity can be depth independent. In case Ω is counterclockwise and $\Delta\Omega$ is clockwise, this is a constant flow to greater depths (or southwards flow) and is

the equivalent of the Sverdrup balanced solution.

Mass is returned to the north by a fast current along the western wall. Beardsley (1969) shows that in case $\tan \alpha << E^{\frac{1}{4}}$, a Stommel (1948) type geostrophic western boundary layer of thickness $E^{\frac{1}{2}}/\tan \alpha$ forms in which vortex shrinking is balanced by Ekman suction. When $\tan \alpha$ approaches $E^{\frac{1}{4}}$, the western boundary layer thins down towards the Stewartson $E^{\frac{1}{4}}$ layer. In this case the diffusion of vorticity from the side wall is balanced by orographic vortex stretching as well as by Ekman-layer suction. When $\tan \alpha >> E^{\frac{1}{4}}$ the flow is analogous to the Munk and Carrier (1950) model with lateral friction.

Rotating a rigid lid simulates a constant wind-stress curl, with uniform vertical velocity out of the top Ekman layer. This effect could as well have been simulated by a uniform distribution of sources of mass at a non-rotating top boundary (Baker, 1973). Wind-stress patterns are not always describable by a constant curl. Any jet such as the Findlater or 'low-level' jet over the Arabian Sea could better be described as a concentrated region of anticyclonic curl adjacent to another concentrated region of cyclonic curl. Such a wind-stress pattern is simulated by a line of sources adjacent to a line of sinks in a porous upper boundary. Figure 1(d) and figure 7(b) demonstrate this.

In the case of a two layer fluid it was found in these experiments that the lower layer has mean velocities approximately two orders of magnitude smaller than the upper layer velocities. Thus, the assumption made in many theories that there is no stress transmitted across the interface appears to be most reasonable. A Sverdrup interior and a Stommel type western boundary layer is then a possible solution for the upper layer. The interface becomes distorted in such a way as to prevent pressure gradients in the lower layer, the slope of the interface being proportional to the interior velocity of the upper layer in accordance with the Witte-Margules formula. The change in upper layer depth produced by such distortion of the interface does not affect the vorticity of the upper layer since the geostrophic flow is perpendicular to the depth gradient. This being the case, distortions of the interface should not be thought of as contributing to the "β-effect".

Lower layer motions are, however, possible in the western boundary layer even for steady flow. Welander (1968) shows a recirculating flow confined to the western boundary lower layer if the northward gradient of f/h is positive, where f is the Coriolis parameter, h is the lower layer depth.

For a two-layer laboratory model governed by Ekman-type dynamics, the following is a convenient starting point.

3. Theoretical basis for the two-layer model

For steady linear flow, the vorticity equation in each layer can be shown to be (Hart, 1972)

$$\underset{\sim}{V}_1 \cdot \underset{\sim}{\nabla} H_T - \frac{E_1^{\frac{1}{2}}}{2} (\nabla^2 P_1 - 2) + \frac{E_1^{\frac{1}{2}}}{2} \frac{\varkappa}{1+\varkappa} (\nabla^2 P_2 - \nabla^2 P_1) = 0 \quad (1)$$

$$\underset{\sim}{V}_2 \cdot \underset{\sim}{\nabla} H_B - \frac{E_2^{\frac{1}{2}}}{2} \nabla^2 P_2 - \frac{E_2^{\frac{1}{2}}}{2} \frac{1}{1+\varkappa} (\nabla^2 P_2 - \nabla^2 P_1) = 0 \quad (2)$$

where $\underset{\sim}{V}_1$, $\underset{\sim}{V}_2$, are the upper, lower layer velocities respectively, P_1, P_2 are the upper, lower layer geostrophic stream functions respectively, H_T is the shape function of the top lid, H_B of the bottom. Here $\varkappa = \nu_1 / \nu_2$ and we shall take

$$H_T = -y \tan \alpha_1$$

$$H_B = y \tan \alpha_2$$

The first term in equation (1) represents the orographically induced vertical velocity resulting from geostrophic flow along the top boundary. The second term is the Ekman suction at the top associated with interior vorticity, the third is the vertical velocity resulting from Ekman layer divergence. The fourth and fifth terms represent Ekman suction at the interface associated with the interior vorticities of the lower and of the upper layers. The Froude number is assumed to be small and vortex stretching as columns of fluid move

over the parabolic mean interface is neglected. For a 10 cm radius tank rotating at 20 rpm, the interface is only approximately 1 mm higher at the rim than at the center. This may be compared to the change in height of 2 cm due to the slope of the lid.

If we take $\nu_1 = \nu_2$ the above equations become

$$(\nabla^2 + \beta_1 \frac{\partial}{\partial x}) P_1 - 1/3\nabla^2 P_2 = 4/3 \qquad (3)$$

$$(\nabla^2 + \beta_2 \frac{\partial}{\partial x}) P_2 - 1/3\nabla^2 P_1 = 0 \qquad (4)$$

where we have defined

$$\beta_1 = 4/3 \frac{\tan\alpha_1}{E_1^{\frac{1}{2}}}$$

$$\beta_2 = 4/3 \frac{\tan\alpha_2}{E_2^{\frac{1}{2}}}$$

For a flat-bottomed ocean we would chose a model with $\beta_1 = \beta_2$. However β_2 could be varied to represent different bottom topographies. For example, if β_2 is chosen zero, we find the upper layer equation reduces to Stommel's equation for a homogeneous fluid, while the lower layer is motionless everywhere.

The interior balance is given by

$$\beta_1 \frac{\partial P_1}{\partial x} = 4/3$$

$$\beta_2 \frac{\partial P_2}{\partial x} = 0$$

which is the analogue of the Sverdrup interior flow.

The Laplacian terms in (3) and (4) become important in the western boundary layer. Equations for P_1 and P_2 alone can be obtained from (3) and (4), of the form

$$LP_1 = 0$$

$$LP_2 = 0$$

where

$$L = \nabla^4 + \frac{9}{8} (\beta_1 + \beta_2) \nabla^2 \frac{\partial}{\partial x} + \frac{9}{8} \beta_1 \beta_2 \frac{\partial^2}{\partial x^2}$$

If $\tan \alpha_1 = 0E^b$ and $\tan \alpha_2 = 0E^c$, various types of western boundary layers are possible for various magnitudes of b, c. For the upper layer these are generally of the kind discussed by Beardsley (1969), and include a Stommel type western boundary current. In the lower layer, the western boundary region has been shown by Welander (1968) to have various forms depending upon the bottom topography. The present laboratory models include studies with $\tan \alpha_2 =$ 0, 0.04, and 0.84. The second corresponds to $\beta_1 = \beta_2$ for the fluid layer depths chosen.

Table 1 shows the definitions and the range of values of the basic parameters of the laboratory model. It also shows some dimensionless numbers (not all independent). The Ekman number, Rossby number and internal Froude number are the main parameters that are varied in the experiments. In the table are listed the approximate magnitudes of these numbers for large scale oceanic flows. For the laboratory model we chose a range of values that span the oceanic values. In order to keep the Froude number small, we chose a tank of radius L ~ 10cm. Other useful parameters are listed at the bottom of the table.

4. Experimental procedure

For the homogeneous experiments, thymol blue prepared according to the Baker (1966) formula was used as the working fluid. For the two-layer experiments we used thymol blue as the upper layer, and a starch or sugar solution for the lower layer.

To obtain transport in the western boundary current, the tank in figure 1a was used. The velocity profile v(x) was determined by photographing at fixed time intervals the northwards progress of a dye line. The areal transport A is defined as $A = \rho_1 \int_0^{x_0} v(x)dx$ where ρ_1 is the density of the thymol blue, and where x = 0 is at the western wall,

$x = x_0$ is at the center of the gyre. The volume transport T is defined as $T = \rho_1 \int_0^{x_0} v(x)h(x)dx$. The depth h (x) of the upper layer was determined as it varied with x, by suspending fine vertical wires which were marked with a color-coded scale.

The separation experiments were prepared in a similar manner, but using the tank in figure 1c.

The periodic forcing experiments were performed using the tank shown in figure 1d. To simulate the monsoons over the Arabian Sea, the line of sources and sinks was at a thirty degree angle to the east-west. The sources (pumping into the interior) were to the south, the sinks (pumping out of the interior) to the north for the South-west monsoons of summer. The pumping direction was reversed and of smaller magnitude for the North-east monsoons of winter. No attempt was made to simulate the complication of the double branching of the Findlater jet of the summer monsoon. The summer condition was maintained for "three months", corresponding to June, July, and August. One day corresponds to one rotation of the table. The pumps were turned off for "two months", then the reversed pumping corresponding to the winter condition was continued for the following "four months" of November through February. The pumping was stopped for the "three months" of March to May. Then the cycle was repeated for "five years".

5. Observations

5.1 The following are the observations of the first experiment related to northward transport. Figure 2a shows streaklines of the steadily driven flow of a homogeneous fluid, with $\tan \alpha_1 = 0.21$, $\tan \alpha_2 = 0.0$ and $R = -7.35 \times 10^{-2}$. (The negative value of R indicates that $\Delta\Omega$ was in the opposite sense to Ω). It shows the following typical features.

(i) Radial flow across constant depth contours over much of the tank, from shallow to deep for clockwise rotation of the lid. This is analogous to the Sverdrup interior flow to the south.

(ii) This flow is diverted to the west in the rim boundary layer which is several millimeters thick at the eastern part of the rim and becomes several centimeters thick near the western part of the 180° basin.

(iii) The return flow to the north occurs in a fast narrow current along the western boundary. The center of the gyre is far to the west of the center of the basin.

(iv) A stationary topographic Rossby wave is observed where the western boundary current enters the interior. Associated with this is a region of weakly cyclonic flow. There are no instabilities and no time dependence. All of these features are in agreement with Beardsley's homogeneous flows.

For the same slopes and Rossby number, a two layer fluid (fig. 2b) shows similar features, but baroclinic instabilities are now possible. Typical features are:

(i) A westward intensified anticyclonic gyre, with the center of the gyre shifted to the southwest of the location for the homogeneous case.

(ii) The region of cyclonic flow as the western boundary current enters the interior is more pronounced.

(iii) There is instability and time dependence in primarily two scales. There are small waves of wavelength approximately 5mm, which is the baroclinic radius of deformation for this experiment. There is also a larger scale instability, with wavelengths several centimeters. This is evident in the movies, and the conditions for its occurrence have been summarized in the regime diagram below.

(iv) There is a counter-current in the rim boundary layer. This is a highly depth-dependent flow which is strongest just above the interface and which vanishes rapidly with distance above the interface. This counter-current becomes increasingly stronger to the east. It continues along the eastern wall as a northward current and finally enters the interior by flowing cyclonically around the low formed by the topographic Rossby wave.

A summary of the observed instabilities is shown in the regime diagram in figure 3. The curves are taken from Hart's (1972) theory of baroclinic instability in a two-layer fluid, in a circular cylindrical tank. Since ours has western boundaries and boundary currents, different modes may be excited. Also, since Hart had computed the stability curves for only one value of tan α, we used these curves on the plane tan α_1 = 0.21 as well as on the plane tan α_1 = 0.32. On the plane tan α_1 =0.105, we used Hart's curves for tan α_1 = 0. In spite of all these differences, his curves still give a good structure upon which to display and understand our data. The closed circles represent flows which were steady and stable. The half-shaded circles represent points in which only the small (several mm) scale instability was observed. The open circles are those for which both the small (mm) scale and large (cm) scale instabilities were observed.

The measured northwards volume transport T in the western boundary current is plotted against Rossby number in figure 4. The data has been made dimensionless by dividing by Ω and the volume of upper layer fluid in the basin. The lower curve is the transport in a homogeneous fluid, again made dimensionless by dividing by the volume and Ω.

It is seen that as R is increased the transport by the upper layer fluid is considerably greater than the transport by an equal volume of fluid over a rigid bottom. The measured areal transports by homogeneous and upper layer fluid, seen in figure 4b, shows only a small divergence of the two curves at higher Rossby number where the two layer appears to have a somewhat larger areal transport. (The large error bar represents different values obtained in repeated observations, due to the time dependence of the two layer flow at these large values of R.) It is primarily the increased depth of the upper layer just in the region of the fast western boundary flow that results in the greatly increased transport over the homogeneous case.

5.2 The following are the observations related to the second experiment on surfacing and separation.

(i) With the tank in figure 1a and with the lid rotating in a clockwise sense, as in the Trade wind regions, surfacing first occurs on the eastern boundary near the weak cyclonic flow associated with the stationary topographic Rossby wave.

(ii) With the tank in figure 1c, and with the lid rotating in a clockwise sense, as in the anticyclonic part of the westerlies, surfacing of the lower layer occurs on the western boundary, and the fast western boundary current separates from the western boundary before it is forced

to do so by the rim. This is shown in figure 5. The conditions for this surfacing appear to be in agreement with Professor Veronis' theory, but these experiments are still not completed.

5.3 The following are the observations related to the third experiment on the periodic forcing.

The two-layer laboratory model responds to changes in rotation rate or to applied stress in a time short compared to "decades" which applies for a mid-latitude ocean (Veronis & Stommel, 1956). The tank in figure 1a containing 10cm sized basins spins up in about 4 minutes or 80 "days". The tank in figure 1d with a 20 cm basin spins up in about 8 minutes or 160 "days". Furthermore, they can be made to respond in a time on the order of "a month" corresponding to a tropical ocean (Lighthill, 1969). The rapid spin-up of the laboratory model is due to two factors. The first is the presence of a meridional boundary. The second is also related to the geometry of the model; the depth to width ratio of the oceans can never be modelled in a geometrically similar manner in the laboratory. In modelling a steady situation, we could argue that the depth is unimportant since the flow is depth-independent (in each layer). However in the time-dependent situation, the layer depths enter

into the radius of deformation and the baroclinic Rossby wave speed. The radius of deformation

$$\lambda = \frac{\sqrt{g^* H}}{2\,\Omega}, \quad \text{where } H = \frac{d(D-d)}{D},$$

is about 0.5 cm in many of these experiments. Thus the width of the tank is just 40 deformation radii across and can be adjusted at will. In mid-latitudes the deformation radius is about 30 km, while in the tropics this may be about 300 km. Thus a 6,000 km ocean basin in mid-latitudes is 200 deformation radii across, while a similar sized basin in the tropics would be just 20 deformation radii across. At the baroclinic Rossby wave speed of $\beta\lambda^2/4\pi^2$, the travel time across a basin of width L will be

$$\tau = \frac{4\pi^2 f^2}{\beta g^*} \frac{L}{H}$$

where f is the Coriolis parameter. Using $\beta = \frac{\tan \alpha_1}{E_1^{1/2}}$, this gives τ = 80 "days" for the model in figure 1a, and τ = 160 "days" for the model in figure 1d. The response time of 160 "days" or approximately 5 months is too long for simulating the Arabian Sea. However, interesting effects might be expected since the forcing varies with a period of 1 year.

The response of a homogeneous model to constant forcing shown in figure 7a for four different directions of "winds", all of the same magnitude. The response of a two-layer model to a steady westerly jet of the same strength as in 7a is

shown in figure 7b. It consists of an anticyclonic gyre to the South, a cyclonic gyre to the North where there is near-surfacing of the lower layer. It is noted that the response is now time dependent, and there is an interesting relationship between the time dependence in the two gyres. Some of the changing featues are indicated by arrows.

The two-layer model, whose response time is 5 months, is subject to a South west jet and its response is shown after 5 months and after 17 months in figure 7c. A similar situation for a North-east jet of wind is shown in figure 7c.

6. Conclusion

This two-layer laboratory model of wind-driven ocean circulation appears to be capable of simulating some of the gross features observed or expected from theories of the oceanic general circulation. It also produced some unexpected features such as the deep countercurrent along the eastern boundary which is reminiscent of the Davidson Current and the California Undercurrent. Certainly the model allows features not observable in a homogeneous model of ocean circulation.

It is a pleasure to acknowledge the support of this research by the Fluid Dynamics Division of the Office of Naval Research.

References

Baker, D. J. 1966. A technique for the precise measurement of small fluid velocities. J. Fluid Mech. 26, 573.

Baker, D. J. 1971. A source-sink laboratory model of the ocean circulation. Geophys. Fluid Dyn. 2, 17.

Baker, D. J., & Robinson, A. R. 1969. A laboratory model for the general ocean circulation. Phil. Trans. Roy. Soc. London Ser. A 265, 533.

Beardsley, R. C. 1969. A laboratory model of the wind-driven ocean circulation. J. Fluid Mech. 38, 255.

Düing, W. 1970. The Monsoon Regime of the Currents in the Indian Ocean. East-West Center Press, Honolulu.

Findlater, J. 1971. Mean monthly airflow at low levels over the western Indian Ocean. Meteorological Office, Geophysical Memoirs No. 115, London: Her Majesty's Stationery Office.

Greenspan, H. P. 1968. The theory of rotating fluids. Cambridge University Press.

Hart, J. E. 1972. A laboratory study of baroclinic instability. Geophys. Fluid Dyn. 3, 181.

Hart, J. E. 1975. The flow of a two-layer fluid over topography in a polar ocean. J. Phys. Oceanogr. 5, 615.

Krishnamurti, T. N. Northern summer tropical circulations during drought and normal rainfall months. (This volume).

Lighthill, Sir James. 1969. Dynamic response of the Indian Ocean to onset of the Southwest Monsoon. Phil. Trans. Roy. Soc. London Ser. A 265, 45.

Munk, W. H. & Carrier, G. F. 1950. The wind-driven circulation in ocean basins of various shapes. Tellus, 2, 158.

Parsons, A. T. 1969. A two-layer model of Gulf Stream separation. J. Fluid Mech. 38, 511.

Pedlosky, J. & Greenspan, H. P. 1967. A simple laboratory model for the ocean circulation. J. Fluid Mech. 17, 291.

Stommel, H. 1948. The westward intensification of wind-driven ocean currents. Trans. Am. Geoph. Union. 29, 202.

Stommel, H., Arons, A. B. & Faller, A. J. 1958. Some examples of stationary planetary flow patterns in bounded basins. Tellus 10, 179.

Veronis, G. 1973. Large scale ocean circulation. Advances in Applied Mechanics. 13, 1.

Veronis, G. 1973. Model of world ocean circulation: 1. wind-driven, two-layer. J. Mar. Res. 31, 228.

Veronis, G. 1977. Personal communication.

Veronis, G. & Stommel, H. 1956. The action of variable wind stresses on a stratified ocean. J. Mar. Res. 15, 43.

Vonder Haar, T. H. & Oort, A. H. 1973. New estimate of annual poleward energy transport by northern hemisphere oceans. J. Phys. Oceanogr. 3, 169.

Welander, P. 1968. Wind-driven circulation of one- and two-layer oceans of variable depth. Tellus. 20, 1.

Figure captions

Figure 1 (a), (b) Schematic diagram of apparatus used in transport measurements; (c) apparatus used in western boundary current separation studies; (d) apparatus used in periodic monsoonal forcing studies.

Figure 2. Streaklines showing a comparison of the flow pattern for (a) homogeneous and (b) two-layer fluid. All parameters are the same in the two cases except that in (b) $\Delta\rho/\rho = 2.0 \times 10^{-3}$, internal Froude number $f = 20$. The Ekman number for (a) is $E = 2.6 \times 10^{-5}$, and the Rossby number $R = -7.35 \times 10^{-2}$, Froude number $F = 4 \times 10^{-2}$, $\tan \alpha_1 = 0.21$, $\tan \alpha_2 = 0$, for both cases.

(c) As in figure 2(b); arrows indicate the counter current

Figure 3. Regime diagram in the parameter space f (the internal Froude number, $E^{\frac{1}{2}}/R$ (where E is the Ekman number, R the Rossby number), and $\tan \alpha_1$. $\tan \alpha_2 = 0$. The curves are from a theory of baroclinic instability by Hart (1972).

Figure 4 (a) Northward volume transport T of the western boundary current vs Rossby number R.

(b) Northwards areal transport A vs Rossby number R.

Figure 5. Showing non-separated flow (a), and separated flow (b) at the western boundary. All parameters are the same in (a) and in (b) except the upper layer depth is slightly smaller in (b). The tank is that one shown in figure 1(c).

Figure 6. The axis of the Findlater (1971) jet of November is superposed on the dynamic topography (from Düing, 1970) for winter in (a) and the jet of June on the dynamic topography of late summer in (b).

Figure 7 (a) Homogeneous β-plane model showing the oceanic response to various winds; (i) westerlies (ii) south-westerlies (iii) southerlies (iv) east-north-easterlies.

(b) Two-layer β-plane model showing the time-dependent oceanic response to steady westerlies. (i), (ii) and (iii) are at successive times.

(c) Two-layer β-plane model showing the response at (i) 3 months and (ii) at 17 months to steady south-westerlies; (iii) at 3 months and (iv) at 17 months to steady north-easterlies.

APPARATUS

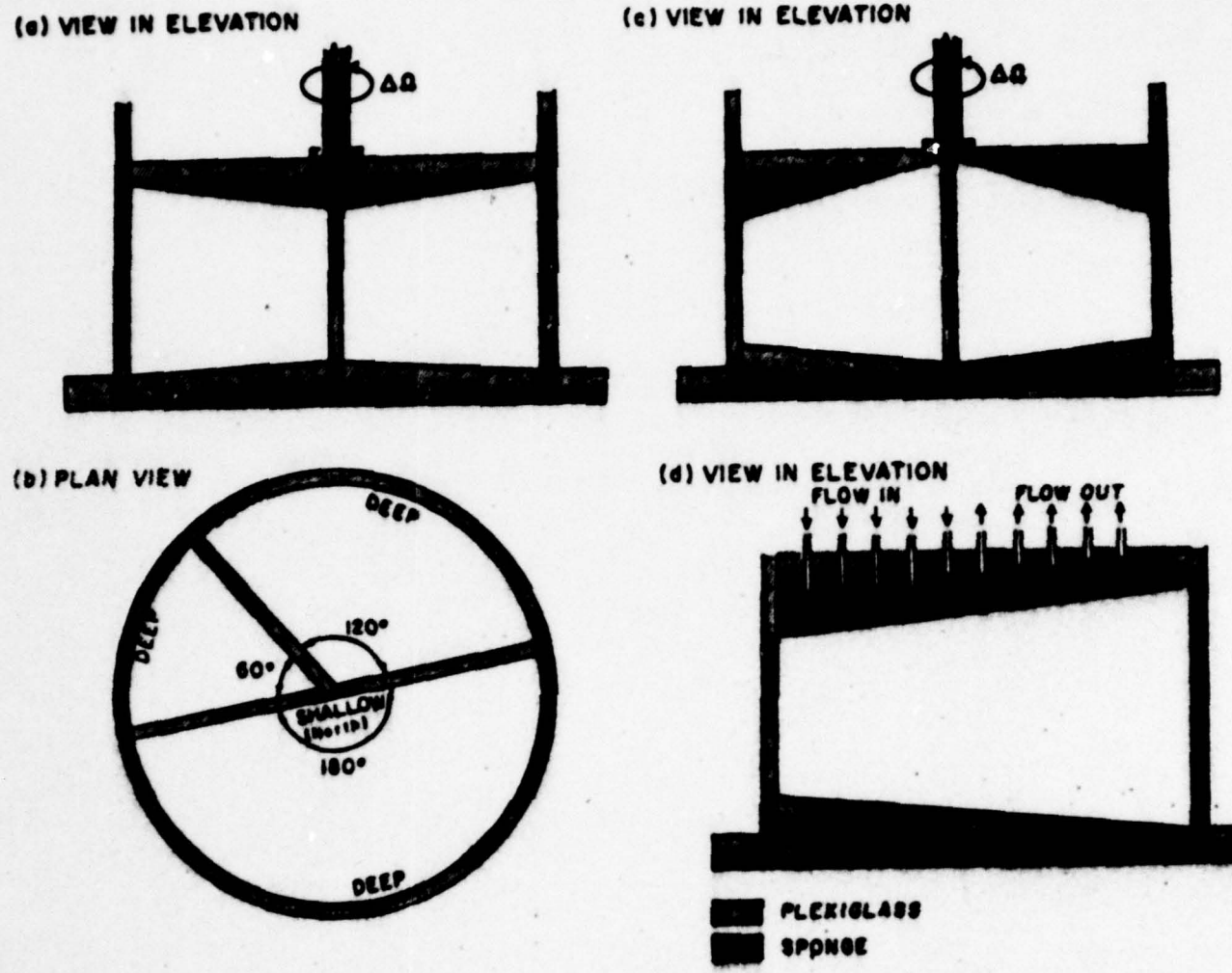

FIGURE 1

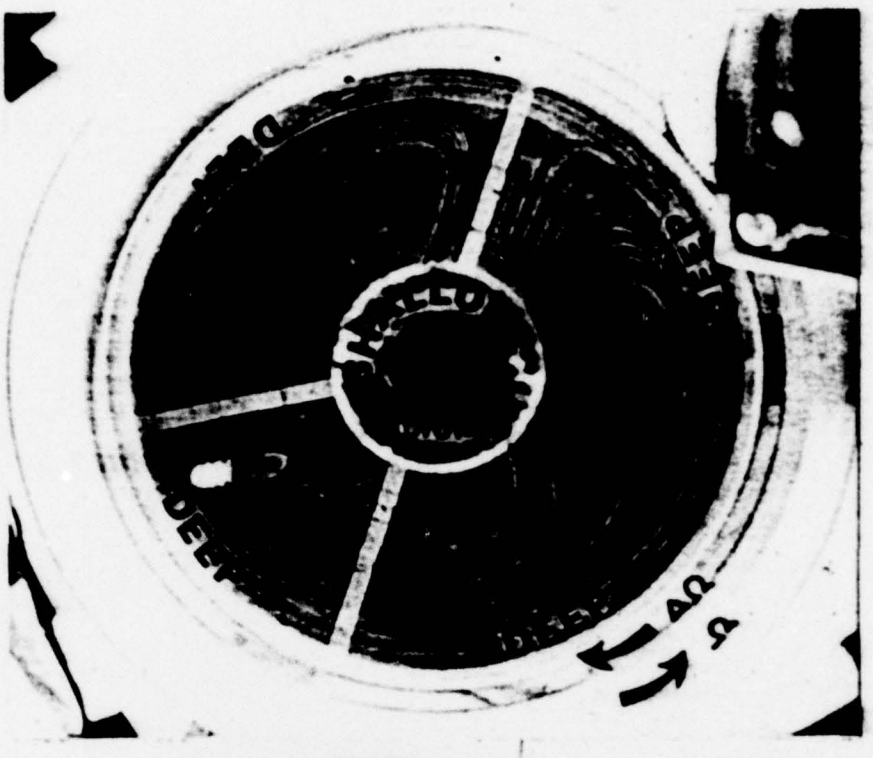

FIGURE 2 (A)

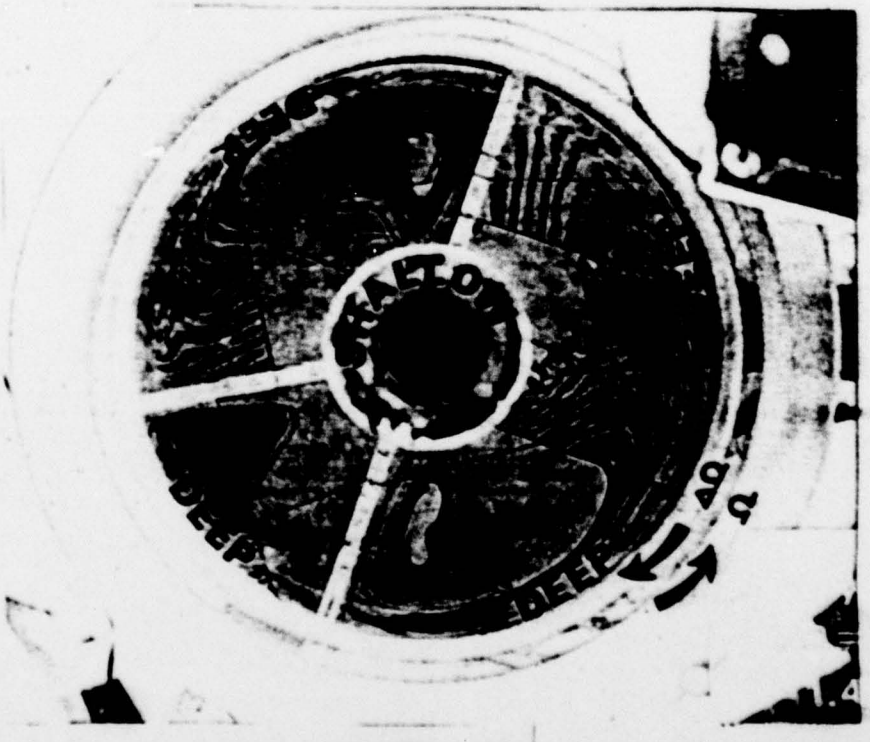

FIGURE 2 (B)

FIGURE 2 (c)

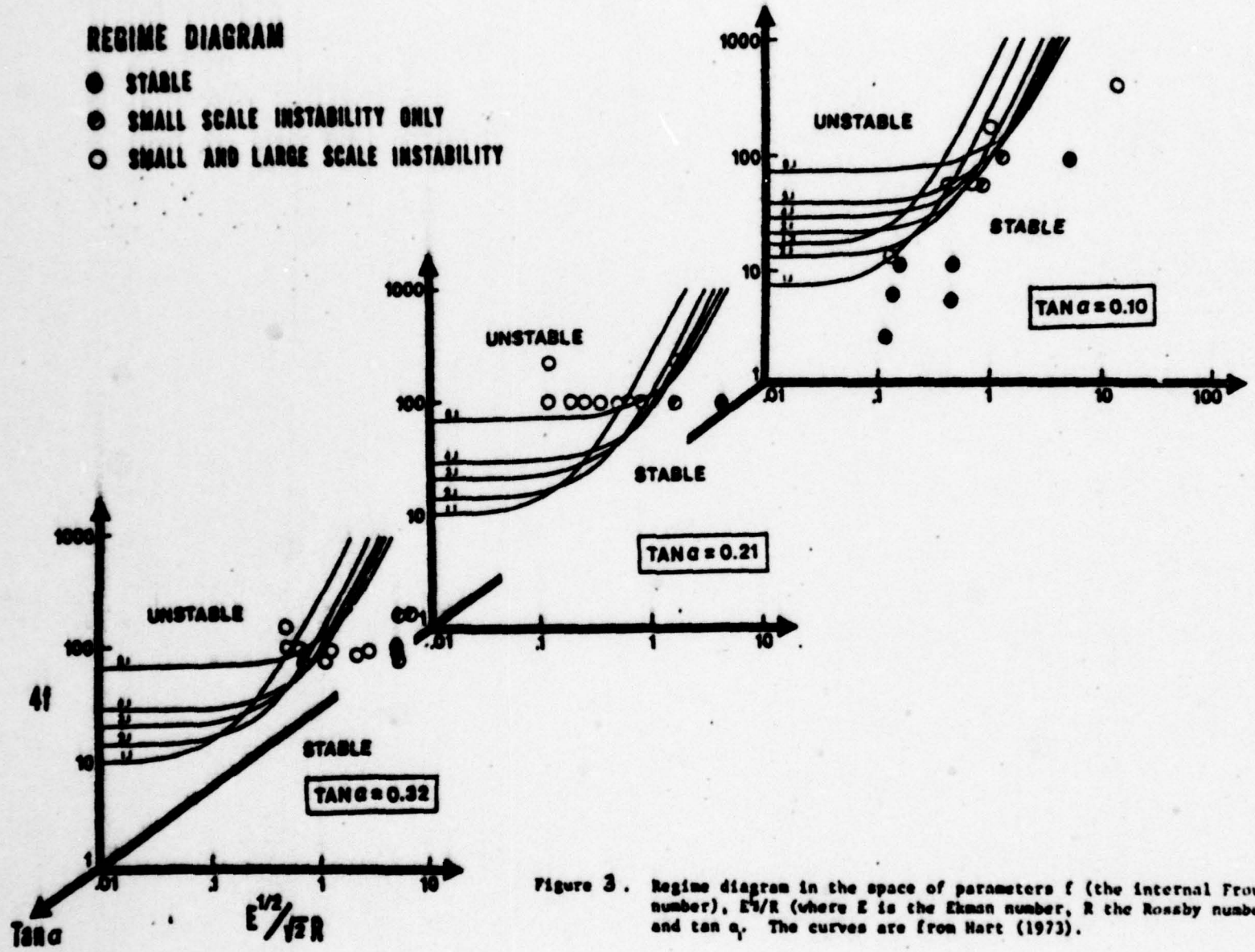

Figure 3. Regime diagram in the space of parameters f (the internal Froude number), $E^{1/2}/R$ (where E is the Ekman number, R the Rossby number), and tan α. The curves are from Hart (1973).

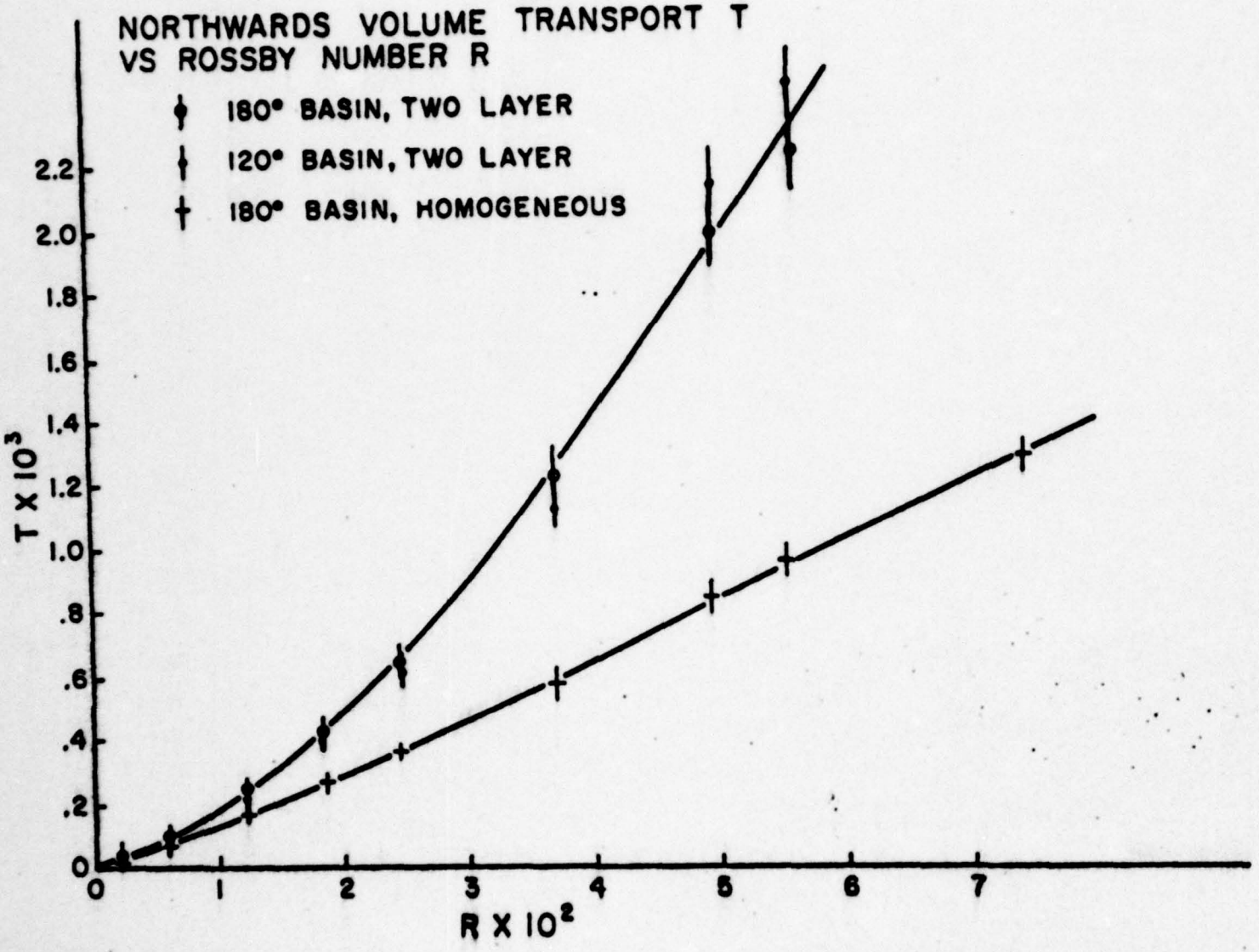
NORTHWARDS VOLUME TRANSPORT T
VS ROSSBY NUMBER R
180° BASIN, TWO LAYER
120° BASIN, TWO LAYER
180° BASIN, HOMOGENEOUS
T X 10³
2.2
2.0
1.8
1.6
1.4
1.2
1.0
.8
.6
.4
.2
0
0
1
2
3
4
5
6
7
R X 10²

FIG. 4 (A)

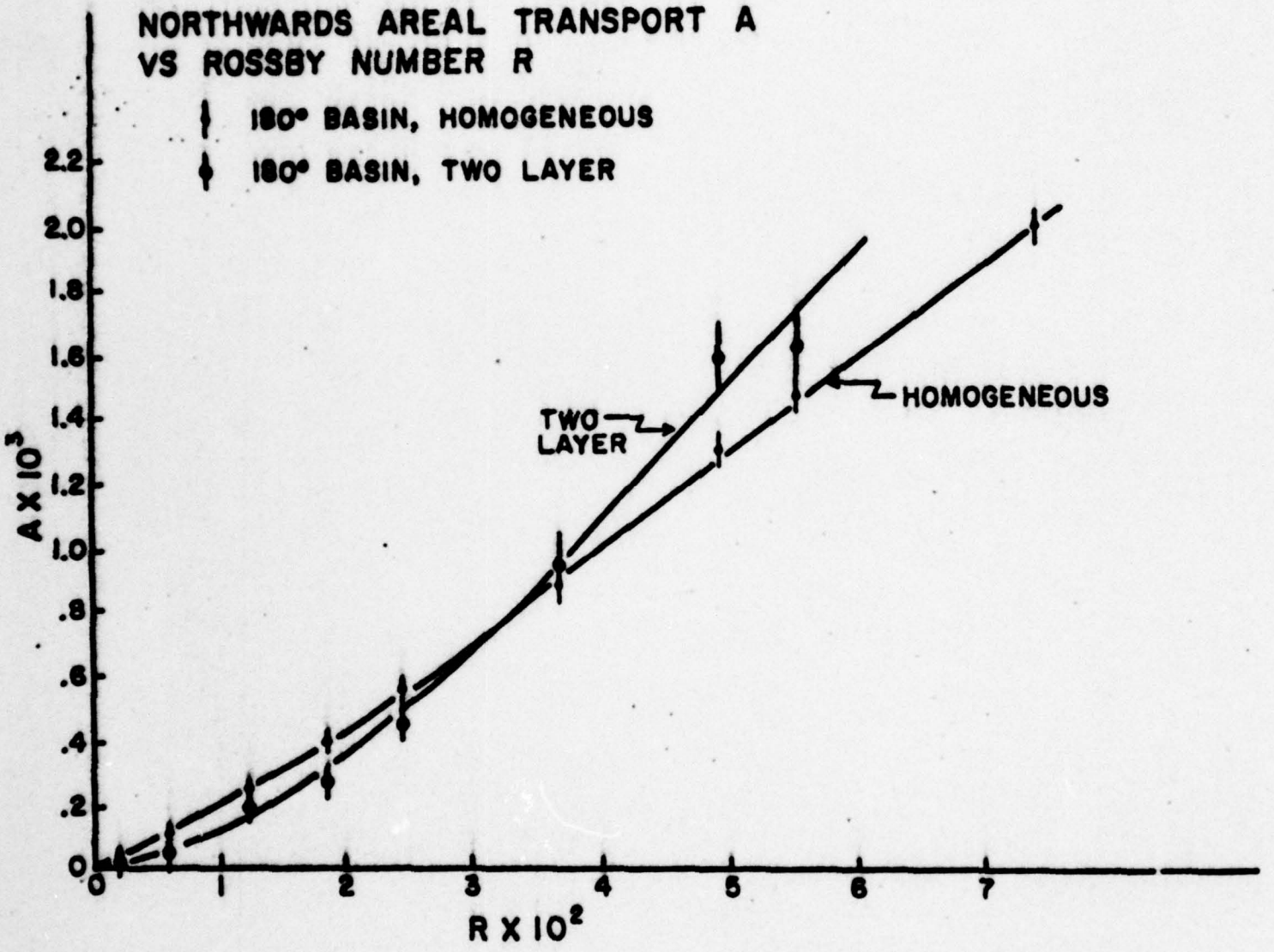
NORTHWARDS AREAL TRANSPORT A
VS ROSSBY NUMBER R
180° BASIN, HOMOGENEOUS
180° BASIN, TWO LAYER
A X 10³
R X 10²
TWO LAYER
HOMOGENEOUS
0
.2
.4
.6
.8
1.0
1.2
1.4
1.6
1.8
2.0
2.2
1
2
3
4
5
6
7

FIG. 4 (a)

FIG. 5 (A)

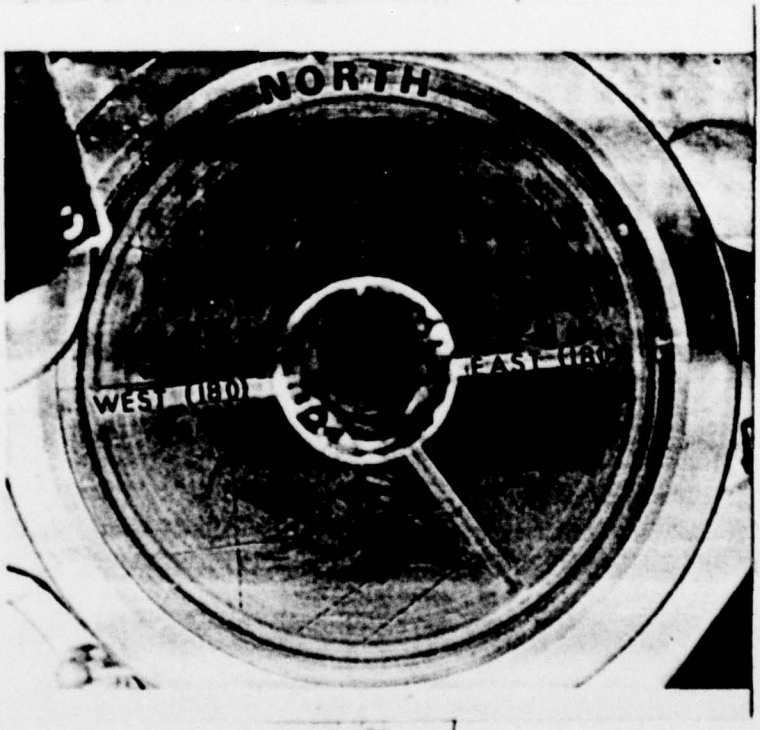

FIG. 5 (B)

FIG. 6 (A)

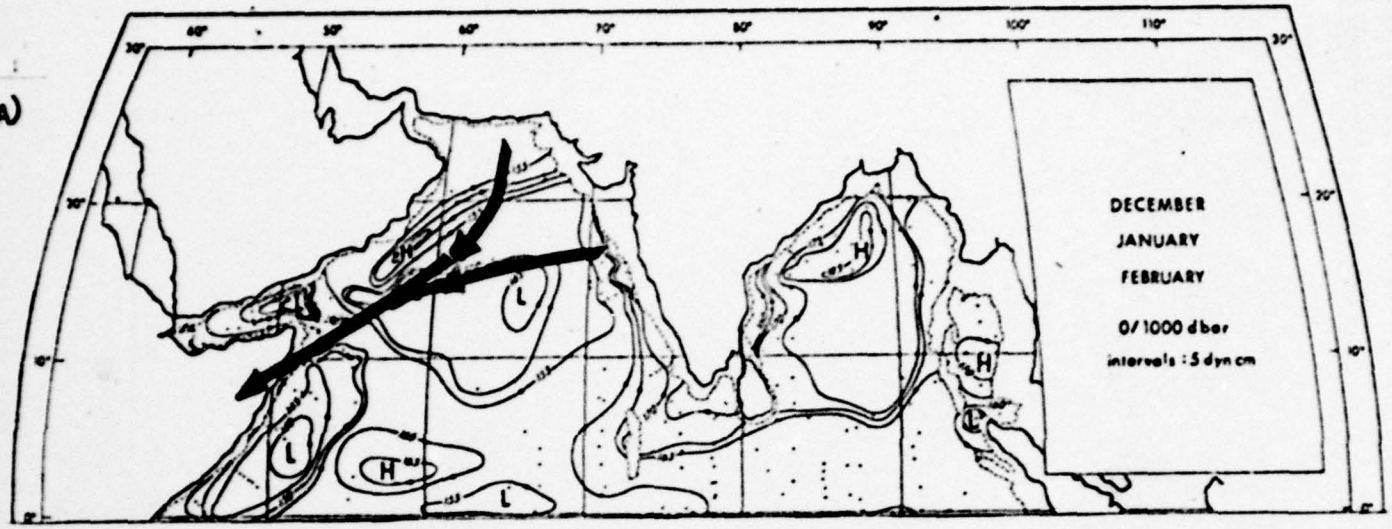
DECEMBER
JANUARY
FEBRUARY
0/1000 dbar
intervals : 5 dyn cm

FIG. 6 (B)

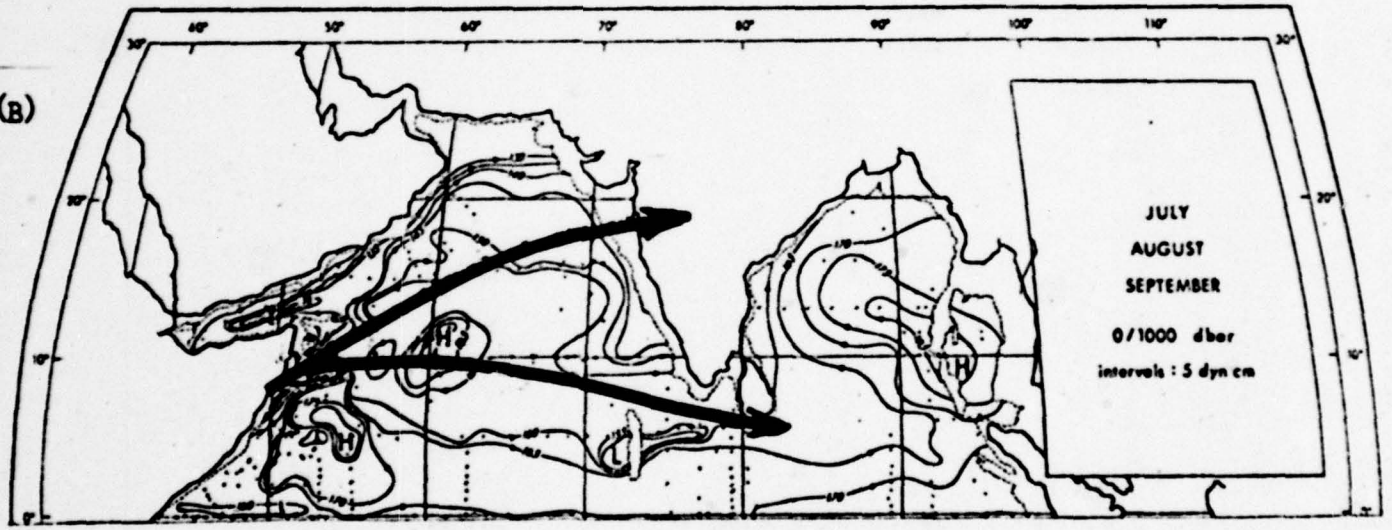
JULY
AUGUST
SEPTEMBER
0/1000 dbar
intervals : 5 dyn cm

OCEANIC RESPONSE TO WINDS

HOMOGENEOUS β PLANE MODEL

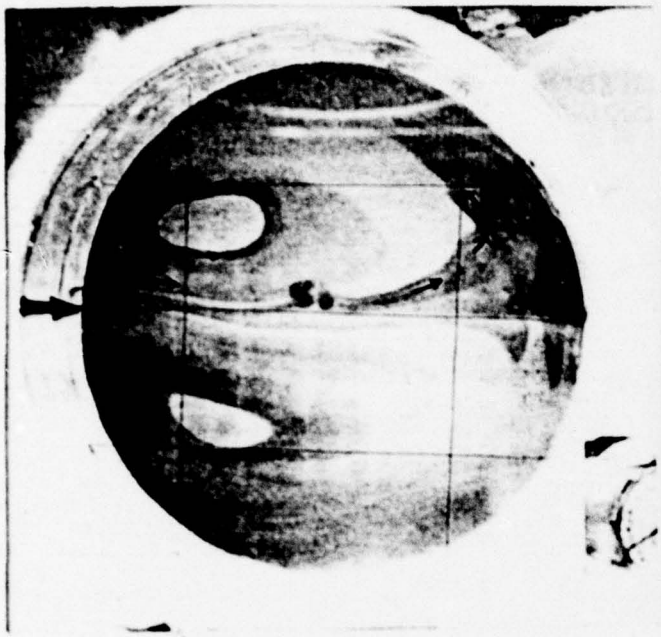

(i) WESTERLIES

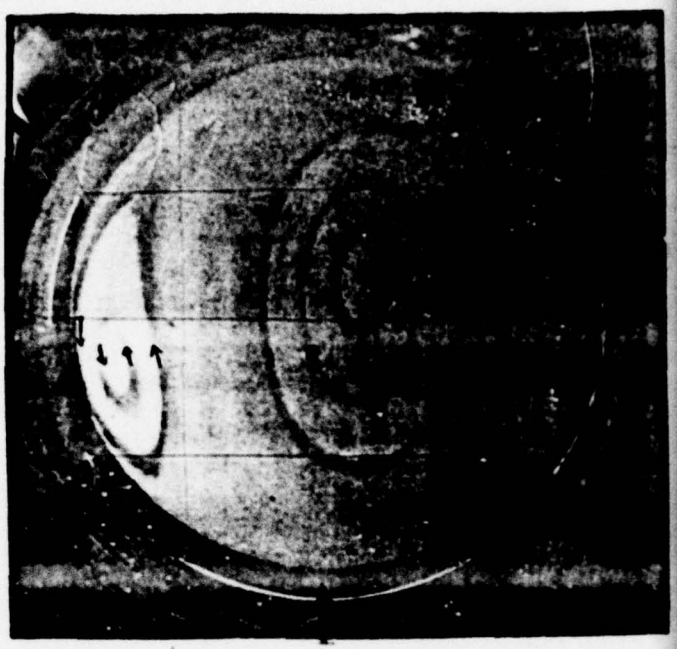

(iii) SOUTHERLIES

(ii) SOUTH-WESTERLIES

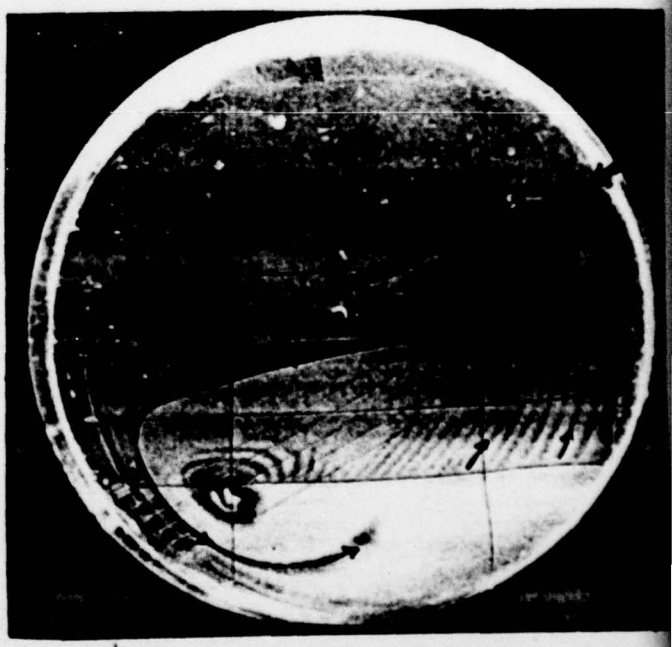

(iv) EAST-NORTH-EASTERLIES

FIGURE 7 (A)

FIGURE 7 (B)

(i)

(iii)

(ii)

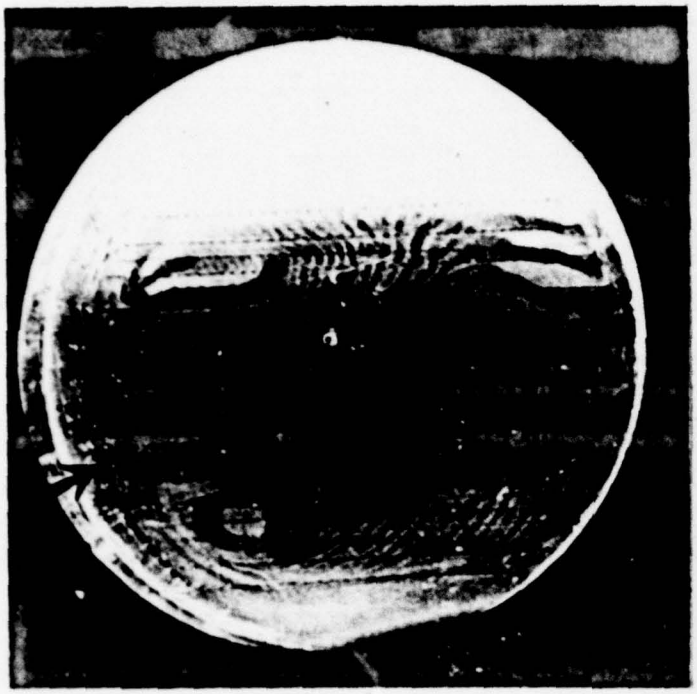

(i)

(iii)

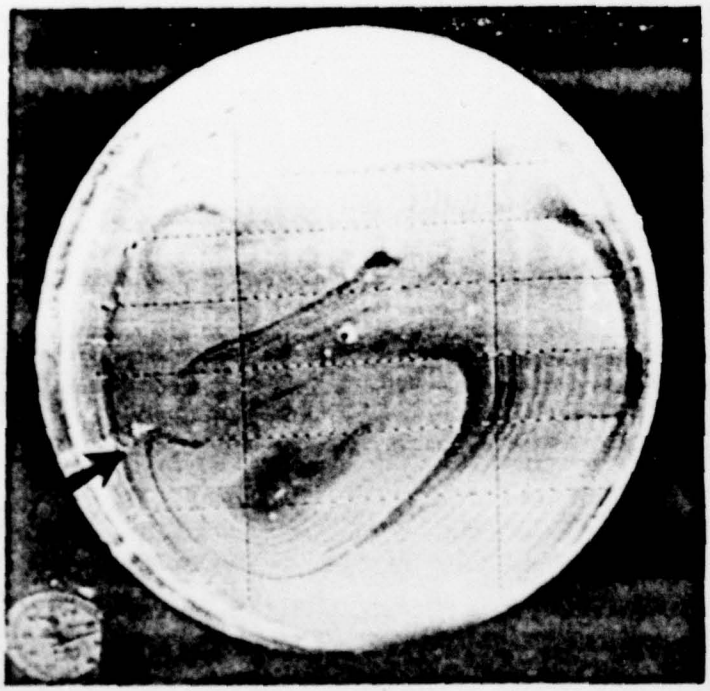

(ii)

(iv)

FIGURE 7 (c)

Security Classification

(Security classification of title, body of abstract and indexing annotation must be entered when the overall report is classified)

1. ORIGINATING ACTIVITY (Corporate author)	2a. REPORT SECURITY CLASSIFICATION
	2b. GROUP

3. REPORT TITLE

Laboratory Modelling of oceanic response to Monsoonal winds

4. DESCRIPTIVE NOTES (Type of report and inclusive dates)

Technical Report

5. AUTHOR(S) (First name, middle initial, last name)

Ruby Krishnamurti

6. REPORT DATE	7a. TOTAL NO. OF PAGES	7b. NO. OF REFS
1978	36	22

8a. CONTRACT OR GRANT NO. N00014-75-C-0877	9a. ORIGINATOR'S REPORT NUMBER(S)
b. PROJECT NO.	No. 15
c.	9b. OTHER REPORT NO(S) (Any other numbers that may be assigned this report)
d.	

10. DISTRIBUTION STATEMENT

This is a technical report to the Office of Naval Research under Contract N00014-75-C-0877 and is intended only for internal distribution. Reproduction in whole or in part is permitted for US Govt.

11. SUPPLEMENTARY NOTES	12. SPONSORING MILITARY ACTIVITY
	Office of Naval Research

13. ABSTRACT

In a laboratory model ocean, fluid in a rotating tank a varying depth is subjected to various stress patterns which simulate both steady and seasonally varying winds, including monsoonal winds. For a certain range of the governing parameters (Rossby number, Ekman number and Froude number), a homogeneous fluid displays steady westward intensified flow. For the same range of parameters a two-layer fluid can have baroclinic instabilities. The parameter range for these instabilities is mapped in a regime diagram. The northward transport of the western boundary current is measured as it varies with imposed wind-stress curl, and is compared with the corresponding values in a homogeneous fluid. The conditions for surfacing of the lower layer is measured as it varies with Rossby number and Froude number. Finally a movie is shown of the response of a two layer fluid to periodically varying winds corresponding to southwest and northeast monsoons.

FORM [illegible]

(PAGE 1)

S/N 0101-807-6811

Security Classification

A-31408